Efficient Tunable Laser Operation of Tm:$KGd(WO_4)_2$ in the Continuous-Wave Regime at Room Temperature

Valentin Petrov, Frank Güell, Jaume Massons, Josefina Gavalda, Rosa Maria Sole, Magdalena Aguilo, Francesc Diaz, and Uwe Griebner

***Abstract*—Tm:$KGd(WO_4)_2$ is studied as a three-level laser on the $^3F_4 \rightarrow {}^3H_6$ transition and a tunable source in the 2-μm spectral range, operating at room temperature. An overall tunability extending from 1790 to 2042 nm is achieved with maximum output powers of 400 mW for an absorbed pump power of 1 W. Various doping levels, pump wavelengths and polarization configurations are compared and the advantages of the monoclinic double tungstates over other Tm-hosts are outlined.**

***Index Terms*—Crystals, lasers, laser tuning, rare earth compounds, solid lasers, thulium, tungsten compounds.**

I. Introduction

THULIUM-DOPED laser materials are emerging as very interesting active media for the 2-μm spectral region due to the possibility for diode pumping near 800 nm and the broad tunability. Potential applications lie in the fields of medicine, laser radar and atmosphere monitoring. The most intensively studied hosts, YAG and YLF, are well known optical materials with mature growth technology. YAG is a cubic crystal with good thermo-mechanical properties (see Table I) while YLF which is uniaxial can provide natural polarization of the laser radiation suppressing thermally induced birefringence. The relatively narrow and weak $^3H_6 \rightarrow {}^3H_4$ absorption line of the Tm^{3+}-ion in YAG and YLF is shifted, however, to shorter wavelengths in comparison to the $^4I_{9/2} \rightarrow {}^4F_{5/2}+{}^2H_{9/2}$ line of the Nd^{3+} ion which poses severe requirements to the existing AlGaAs pump laser diodes. The uniaxial YVO_4 and $GdVO_4$ crystals developed later exhibit in general larger cross sections and broader linewidths as compared to YAG and YLF which is advantageous for *noncritical* diode laser pumping and mode-locking. When doped with Tm they provide the additional advantage of having the absorption line closer to 800 nm (797.5–799 nm [5], [6], [13]) which is better suited for commercially available AlGaAs laser diodes at room temperature. All these positive trends are even more pronounced in the monoclinic double tungstates which are strongly anisotropic biaxial crystals with weaker concentration quenching effects. The latter, in combination with the large cross sections permits the use of relatively thin active elements which additionally reduces the requirements to the pumping source. The advantages of the monoclinic double tungstates for highly efficient, low threshold laser operation with diode pumping are well known in the case of Nd and Yb doping but so far only few laser studies were devoted to Tm-doped double tungstates. We note that the combination of broad fluorescence line, large emission cross section and relatively low upper level lifetime (Table I) is an unique advantage for future experiments on passive mode-locking with such lasers and the generation of femtosecond pulses by an all-solid state laser system tunable in the 2-μm spectral range. Tm-doped double tungstates have an absorption line centered at 800–802 nm [15], [25] with a broader longwave wing very suitable for diode pumping.

The first demonstration of Tm lasing on the $^3F_4 \rightarrow {}^3H_6$ transition in monoclinic double tungstates was realized in 1997 with Xe-flash lamp pumping where Tm:$KY(WO_4)_2$ (Tm:KYW) and Tm:$KGd(WO_4)_2$ (Tm:KGdW) rods sensitized with Er^{3+} and Yb^{3+} operated at cryogenic temperatures and wavelengths of 1920 and 1930 nm, respectively [14]. Soon afterwards continuous-wave (CW) room-temperature operation of highly doped (15%) Tm:KYW was demonstrated with longitudinal Ti:sapphire laser pumping near 800 nm [15]. Codoping of Tm:KYW with Yb^{3+} for InGaAs diode pumping at 980 nm with subsequent excitation transfer was studied in [16] but laser experiments revealed no practical advantages as compared to direct $\approx$ 800 nm pumping by AlGaAs diodes [21]. Passive Q-switching and Raman self-conversion to 2365 nm has also been demonstrated in such lasers [22]. The Tm^{3+} ion in KYW or in $KYb_{0.5}Y_{0.43}Tm_{0.07}(WO_4)_2$ can be excited also at 1064 nm by a Nd:YAG laser through a photon avalanche process [23], [24] as previously realized in Tm:YAG.

KGdW which is isostructural to KYW provides also a strong anisotropy of the physical and optical properties. It was only recently that the spectroscopic properties relevant to laser operation were studied for flux grown Tm:KGdW by a part of the present authors [18], [19], [25] and also by others [20], [26]. While in [20], [26] only unpolarized spectra were presented, the systematic studies in [19] and [25] were performed in the orthogonal frame of the optical indicatrix. In the C2/c space group the lattice parameters of the monoclinic KGdW are $a = 1.0652(4)$ nm, $b = 1.0374(6)$ nm, $c = 0.7582(2)$ nm and $\beta = 130.80(2)^\circ$ with $Z = 4$. The N_P principal optical axis is parallel to the b crystallographic axis. The other principal optical axes N_g and N_m are in the a-c plane with the N_g axis at 21.5°

Manuscript received March 30, 2004; revised May 4, 2004. This work was supported in part by the EU-Commission LIMANS - mbi 000366-7 and Project DT-CRYS, in part by CICyT under Projects MAT2002-04603-C05-03, FiT-070000-2001-477, FiT-070000-2002-461, and FiT-070000-2003-661, and in part by CIRIT under Project 2001SGR00317

V. Petrov and U. Griebner are with Max-Born-Institute for Nonlinear Optics and Ultrafast Spectroscopy, Berlin D-12489, Germany (e-mail: petrov@mbi-berlin.de).

F. Güell, J. Massons, J. Gavalda, R. M. Sole, M. Aguilo, and F. Diaz are with the Department Química Física i Inorgànica, Física i Cristal-lografia de Materials (FiCMA), Universitat Rovira i Virgili, Tarragona E-43005, Catalunya, Spain.

Digital Object Identifier 10.1109/JQE.2004.833193

TABLE I
PROPERTIES OF TM-DOPED LASER CRYSTALS RELEVANT TO 2-μM OPERATION, τ_R: CALCULATED RADIATIVE LIFETIME USING THE JUDD-OFELT (J-O) OR THE CROSS SECTION COMPARISON (C-S) METHODS, τ: MEASURED FLUORESCENCE DECAY TIME. CITATIONS IN THE LAST COLUMN REFER TO THE WHOLE LINE EXCEPT FOR THE FIRST COLUMN

Tm-host, κ: thermal conductivity, ΔE: ground state splitting	σ_e: emission cross section [10^{-20}cm^2]	λ_e: emission wavelength [nm]	τ_r [ms]	τ [ms]	$\sigma_e \times \tau$ [10^{-20}cm^{2}ms]	Tm-doping [Ref.]
$Y_3Al_5O_{12}$ (YAG) κ=10.3-13 $Wm^{-1}K^{-1}$ [1] ΔE=580 cm^{-1} [2]	0.22	2011	12.3 (C-S)	10.5	2.31	1% [2]
$LiYF_4$ (YLF) κ=4.3-7.2 $Wm^{-1}K^{-1}$ [1] ΔE=360 cm^{-1} [2]	0.33 (E⊥c)	1902 (E⊥c)	11.9 (C-S)	15.6	5.15	1% [2]
	0.35 (E//c)	1880 (E//c)			5.46	
	0.24 (E⊥c)	1910 (E⊥c)	15.0 (C-S)	15.6	3.74	0.5% [28]
	0.38 (E//c)	1880 (E//c)			5.93	
YVO_4 κ=5.1-9.4 $Wm^{-1}K^{-1}$ [3,4,12] ΔE=332-367 cm^{-1} [10]	2.7 (E⊥c)	1800	0.695 (J-O)	0.75-0.8	2.03-2.16	5% [5,6,7]*
	1.6 (E//c)				1.2-1.28	
	-	-	1.29 (J-O)	1.03	-	1% [8,9]
	2.60 (E//c)	1805	1.165 (J-O)	-	-	0.5% [3,4,10]
	1.73 (E⊥c)	1804			-	
$GdVO_4$ κ=9.7-12.3 $Wm^{-1}K^{-1}$ [11,12]	-	1830	-	0.93	-	2.5% [13]
$KY(WO_4)_2$ (KYW) κ≈3 $Wm^{-1}K^{-1}$ [14]	1.9 (E in N_m-N_g)	1850	-	1.47	2.79	15% [15]
	2.8-3.8 (E//*a'*)	1820	0.99 (C-S)	1.25	3.5-4.75	3% [16]
$KGd(WO_4)_2$ (KGdW) κ=2.6-3.8 $Wm^{-1}K^{-1}$ [17] ΔE=460 cm^{-1} [18]	3.27 (E//N_m)	1834	1.31 (C-S)	1.76	5.76	3% [19], this work
	1.64 (E//N_p)**	1824**			2.89	
	1.56 (unpol)	1825	0.8 (J-O)	-	-	3.5% [20]

*It is suspected that the two polarizations were erroneously exchanged in [5,6] since the same authors obtained laser oscillation for π-polarization, but this could not be reliably checked, see more recent literature on Tm:YVO_4 [3,4,10].
**Emission wavelength and cross section correspond to the second maximum in Fig. 1.

from the c crystallographic axis in the clockwise direction. These three orthogonal axes are defined by the standard convention for the principal refractive indices: $n_p < n_m < n_g$. An updated value of the maximum emission cross section of $\sigma_e = 3.27 \times 10^{-20}\text{cm}^2$ at 1834 nm (Table I) was calculated now for polarization parallel to N_m by the reciprocity method from the absorption spectra presented in Fig. 1. The measured decay time τ of the upper laser level ($^3F_4$) population was estimated to decrease from 1710 to only 1530 μs for Tm doping varying from 1 to 10% [19]. The radiative lifetime of 1.31 ms was calculated for Table I from the updated emission cross sections (cross section comparison method) which is equivalent to the requirement that the Fuechtbauer–Ladenburg and the reciprocity methods provide close results for the cross sections (the partition functions and zero-line energy used in the calculation can be found in [19]). This approach follows closely the strategy adopted in the review [2] for comparison of various Tm-hosts. The deviation of τ_r from the measured τ is a measure for the reliability of the spectroscopic data. Note that the shorter radiative upper level lifetime τ_r calculated in [20] for a 3.5% Tm-doped KGdW (Table I) was derived from unpolarized spectral measurements by the Judd–Ofelt theory which was shown in [27] to be less accurate in the case of the Tm-ion. It is difficult to compare the results of [19] and those depicted in Fig. 1. to similar estimations in Tm:KYW because of the different methods and crystal orientations used. Thus, for instance, in [19] and in the present work the reciprocity method was used to calculate the emission cross section σ_e from the measured absorption. In contrast, in [15] the emission cross section (for unspecified polarization in the a-c plane of 15%-doped Tm:KYW, see Table I) was estimated following

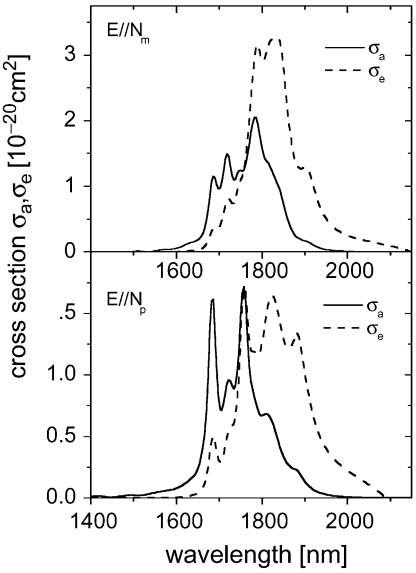

Fig. 1. Absorption cross sections σ_a corresponding to the $^3H_6 \rightarrow {}^3F_4$ transition recorded for polarizations $E//N_m$ and $E//N_p$ (solid lines) with a 3% Tm-doped KGdW and emission cross sections σ_e (dashed lines) calculated by the reciprocity method.

the Fuechtbauer–Ladenburg method of calculating it from measured spectral density of the fluorescence and assuming $\tau_r = \tau$. It was shown in [16] that the Fuechtbauer–Ladenburg method results in larger ($\sigma_e = 3.8 \times 10^{-20}$ cm^2) maximum emission cross section for Tm:KYW than the reciprocity method ($\sigma_e = 2.8 \times 10^{-20}$ cm^2) which was used also by us. Having in mind the results in [19] and in Fig. 1, it can be suggested that this discrepancy is caused by overestimation of the

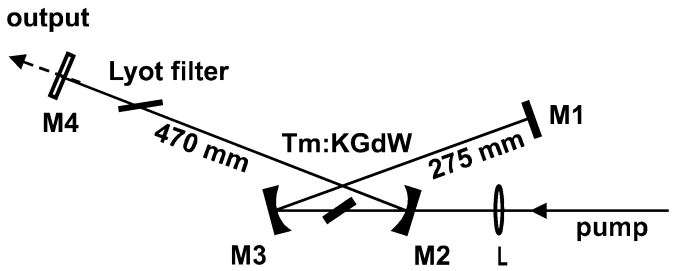

Fig. 2. Laser setup. L: f =70-mm AR-coated lens, M1: plane total reflector, M2-M3: RC = −100-mm mirrors, M4: plane output coupler.

emission cross section when using the Fuechtbauer–Ladenburg method by assuming too low τ_r which in turn is a consequence of the assumption of equal absorption cross sections for $E//a'$ and $E//b$ in [16]. When comparing Tm:KGdW to Tm:KYW it should be taken into account that the estimations in [16] were performed for a polarization $E//a'$, i.e., at ≈24° (see [17]) from the N_m axis in the a-c plane (Table I). From the data in Table I and the inconsistencies in the literature outlined it can be concluded that the emission cross sections estimated for Tm:KGdW and $E//N_m$ in [19] and upgraded in Fig. 1 and Table I agree almost perfectly with those obtained in [16] by the same method for Tm:KYW. As for the upper level lifetime τ measured for Tm:KGdW in [19], it agrees very well with the value obtained in [15] for Tm:KYW. Therefore, the Tm-doped monoclinic tungstates turn out to possess the largest emission cross sections of all crystals included in Table I and, as can be seen for Tm:KGdW, exhibit larger ground state splitting than Tm:YVO_4 or Tm:YLF which is an important advantage in the three-level laser operation scheme.

In this work, we investigate the CW laser characteristics of Tm-doped KGdW at room temperature using a tunable pump source in order to compare both polarizations $E//N_m$ and $E//N_p$ with special emphasis on the tuning behavior for future passive mode-locking experiments. Note that for polarization parallel to the N_g axis the emission cross section is about six and three times lower than for polarization parallel to the N_m and N_p axes, respectively [19], and consequently such orientation is not attractive for laser operation.

II. Experimental Setup and Sample Parameters

An astigmatically compensated X-type cavity with a total length of 85 cm (Fig. 2) was used in the present work in contrast to previous studies with Tm:KYW which relied on simple two-mirror resonators [14], [15], [21]–[22]. It allows easy insertion of tuning elements and also extension with mode-locking devices. Mirrors M1-M3 were highly reflecting (HR > 99.9%) from 1800 to 2075 nm and AR-coated on the rear side for high transmission from 780 to 1020 nm. In the studied tunability ranges, the used output couplers (OC) (M4 in Fig. 2) had transmissions of 4.8–5.6% ($T_{\rm OC}$ = 5%), 2.75–3.5% ($T_{\rm OC}$ = 3%), and 1.45–1.7% ($T_{\rm OC}$ = 1.5 %). As a pump source we employed a Ti:sapphire laser delivering an output power of more than 3 W when pumped with 20 W of an all-lines Ar-ion laser. In the position of the active element (Fig. 2), the pump spot had a gaussian waist of w_P = 37 μm. The Ti:sapphire laser was tunable by translating the slit positioned in the middle of a standard four-prism sequence used for negative group velocity dispersion when operated in the mode-locking regime but it was applied here only in the CW mode of operation. The output linewidth was 0.3 nm but, without additional stabilization, slow wavelength fluctuations as large as 1 nm occurred.

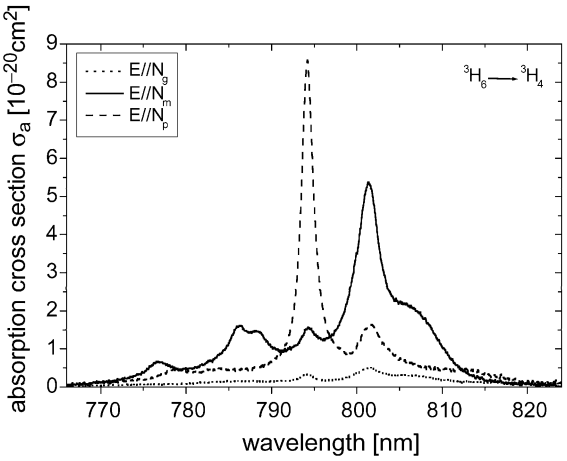

Fig. 3. Absorption cross section of Tm: KGdW for the $^3H_6 \rightarrow {}^3H_4$ transition and the three polarizations.

Uncoated KGdW samples of 5%, 7.5%, and 10% mol of Tm_2O_3 substituting Gd_2O_3 in the solution were available for the present experiments whose exact composition is specified in [25]. They were grown with good optical quality at the Rovira i Virgili University, Tarragona, Spain. Without special cooling the 7.5% and 10% Tm-doped KGdW samples cracked at absorbed powers $P_{\rm abs}$ exceeding 1.5 and 1 W, respectively. The reasons for the fracture are still not well understood but they may be probably associated with the anisotropy in the thermal expansion [28]. That is why we restricted the present study to doping levels of 5% and 7.5% and absorbed powers of up to $P_{\rm abs}$ ≈1 W. The three samples studied were (1) a d =1.71-mm-thick plate with 5% Tm-doping [N = 2.57 10^{20} ions/cm^3 Tm concentration corresponding to a stoichiometric composition of $KGd_{0.959}Tm_{0.041}(WO_4)_2$], cut and oriented for laser polarization parallel to N_m and propagation along the N_p axis, (2) a $d = 1.58$-mm-thick plate of the same composition, cut and oriented for laser polarization parallel to N_p and propagation along the N_m axis, and (3) a d = 1.92-mm-thick plate with 7.5% Tm doping [N = 3.78 10^{20}ions/cm^{3}Tm concentration corresponding to a stoichiometric composition of $KGd_{0.939}Tm_{0.061}(WO_4)_2$], cut and oriented for laser polarization parallel to N_m and propagation along the N_p axis.

The measured absorption cross sections for the $^3H_6 \rightarrow {}^3H_4$ transition in Tm:KGdW are shown in Fig. 3 for the three polarizations. Efficient pumping for laser oscillation at the $^3F_4 \rightarrow {}^3H_6$ transition in a quasithree-level scheme can be achieved near 794 and 802 nm for $E//N_p$ and near 801.5 nm for $E//N_m$. With the present setup and at the maximum absorbed powers used, we observed relatively weak (as compared to the results with Tm:KYW [15]) saturation of the absorption (bleaching) which was strongest (about 20% transmission) in the case of 794-nm pumping of the 5% Tm-doped sample for $E//N_p$. The saturation effect is inversely proportional to the absorption cross section and we observed practically no

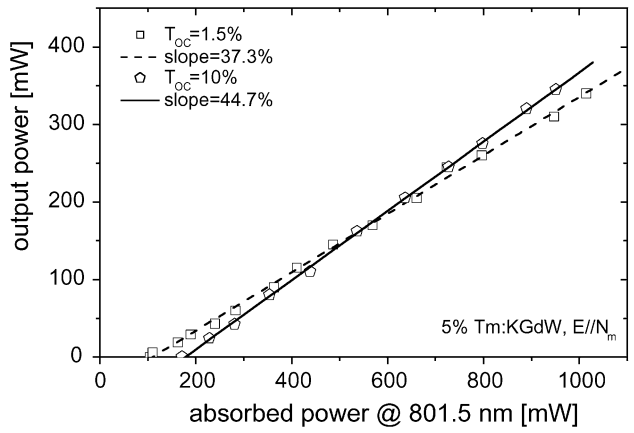

Fig. 4. Input-output characteristics of the 5% Tm:KGdW laser for polarization parallel to the N_m principal optical axis. See Fig. 7 for the oscillation wavelengths.

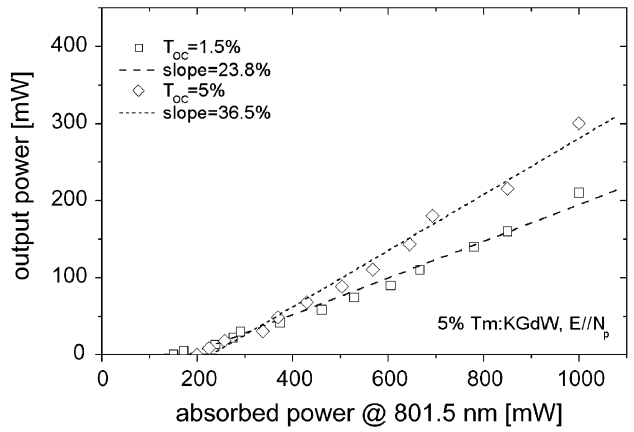

Fig. 5. Input-output characteristics of the 5% Tm:KGdW laser for polarization parallel to the N_m principal optical axis. See Fig. 8 for the oscillation wavelengths.

saturation for the same sample and polarization when pumping at 802 nm. Although in the case of $E//N_p$ the 794-nm absorption line is much stronger (Fig. 3) we concentrated more on the 802-nm absorption line because it is broader and more suitable for diode pumping. Note that in the case $E//N_m$ the broad absorption line possesses an almost flat longwave arm which is ideal for AlGaAs laser diode pumping with reduced requirements for wavelength (temperature) stabilization.

III. Results and Discussion

Fig. 4 and 5 show the dependence of the laser output power on the absorbed pump power at 801.5 nm for the 5% Tm-doped KGdW samples cut for $E//N_m$ and $E//N_p$, respectively. For Fig. 4 ($E//N_m$) the threshold absorbed pump power was 70 mW ($T_{\rm OC} = 1.5\%$) and 130 mW ($T_{\rm OC} = 10\%$). The output couplers with $T_{\rm OC} = 3\%$ and 5% provided similar results with slope efficiencies equal to 41.5% and 43%, respectively. The maximum output power (400 mW) for $E//N_m$ and $P_{\rm abs} = 1$ W (1.35 W of pump power in front of L in Fig. 2) was obtained with $T_{\rm OC} = 3\%$ which is a representative figure for the additional resonator round trip losses. The corresponding pump efficiency with respect to the absorbed power (40%) is very close to the quantum efficiency limit (42%) for a

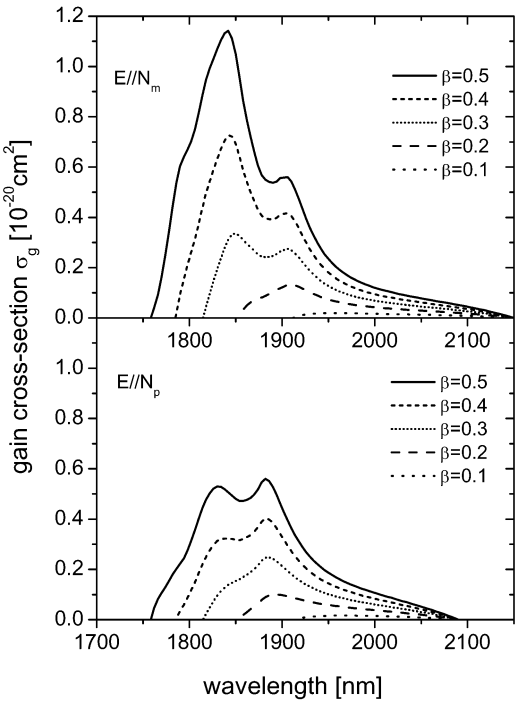

Fig. 6. Inversion dependent gain cross sections $\sigma_g = \beta\sigma_e - (1-\beta)\sigma_a$ for polarization parallel to the N_m and N_p principal optical axes. The absorption (σ_a) and emission (σ_e) cross sections used are from Fig. 1.

lasing wavelength of 1924 nm if cross relaxation processes are neglected (otherwise the quantum efficiency limit amounts to 82%). While quantum efficiency close to 2 can be really expected at high doping levels [15] more quantitative estimations for Tm:KYW [16] and also for Tm:KGdW [19] show that the cross-relaxation self-quenching process for the $^3H_4$ state starts from Tm-concentrations exceeding 3% which means that for the present doping levels the quantum efficiency should have an intermediate value between 1 and 2. Both, thresholds and efficiencies achieved for $E//N_m$ in Fig. 4 are comparable to the results demonstrated previously with Tm:KYW [15], [21].

The output powers obtained for $E//N_p$ were in general lower (by 30% to 50% depending on $T_{\rm OC}$). For Fig. 5 ($E//N_p$) the threshold absorbed pump power was 120 mW ($T_{\rm OC} = 1.5\%$) and 180 mW ($T_{\rm OC} = 5\%$). In addition to the data in Fig. 5, similar results were obtained for $T_{\rm OC} = 3\%$ with a slope efficiency of 34%. It is the first time Tm-generation is obtained for $E//N_p$ in a monoclinic double tungstate. In all previous works [14], [15], [21], [22], the active elements were cut along the b-axis. The increased thresholds and the lower output powers indicate smaller gain cross section in the case $E//N_p$ as compared to $E//N_m$ as could be expected from spectroscopic studies [19]. The inversion dependent gain cross sections for both polarizations are plotted in Fig. 6 for several values of the parameter β corresponding to the ratio of the excited ions density to the total Tm-ion density. It can be seen that in general the gain for $E//N_m$ is higher.

While the incident pump power (in front of L in Fig. 2) necessary to achieve $P_{\rm abs} = 1$ W was as high as 2 W for $E//N_p$ and a pump wavelength of 801.5 nm, this power could be reduced to 1.35 W for pumping at 794 nm. In terms of maximum output powers, thresholds and slope efficiencies, however, the

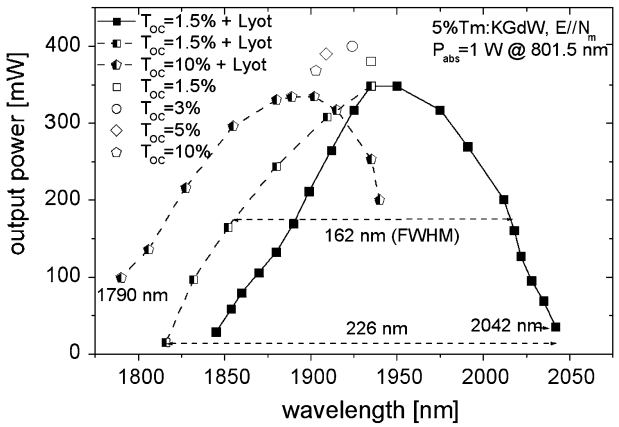

Fig. 7. Continuous tunability for $T_{\rm OC} = 1.5\%$ (solid squares) and discrete tuning for $T_{\rm OC} = 1.5\%$ (half-filled squares) and $T_{\rm OC} = 10\%$ (half-filled pentagons) achieved with the 5% Tm:KGdW sample for $E//N_m$ and pumping at 801.5 nm. For comparison the generation wavelengths and output powers obtained without tuning element in the cavity are given for the four output couplers used (open symbols) and the same absorbed pump power $P_{\rm abs} = 1$ W.

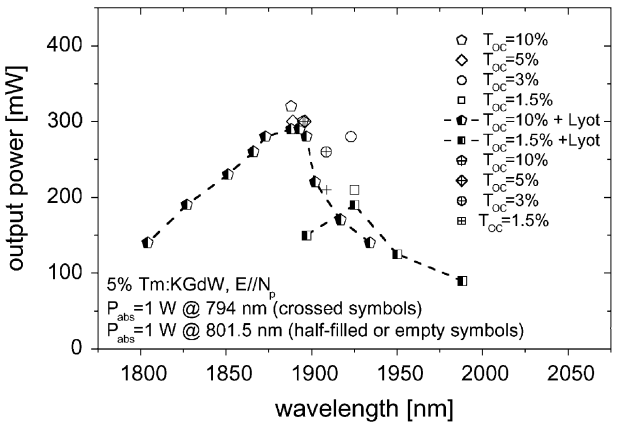

Fig. 8. Discrete tunability with the 5% Tm:KGdW sample for $E//N_p$, pumped at 801.5 nm achieved with $T_{\rm OC} = 1.5\%$ (half-filled squares) and 10% (half-filled pentagons). For comparison the generation wavelengths and output powers obtained without tuning element in the cavity are given for the four output couplers used, the two pump wavelengths of 801.5 (open symbols) and 794 nm (crossed symbols), and the same absorbed pump power $P_{\rm abs} = 1$ W.

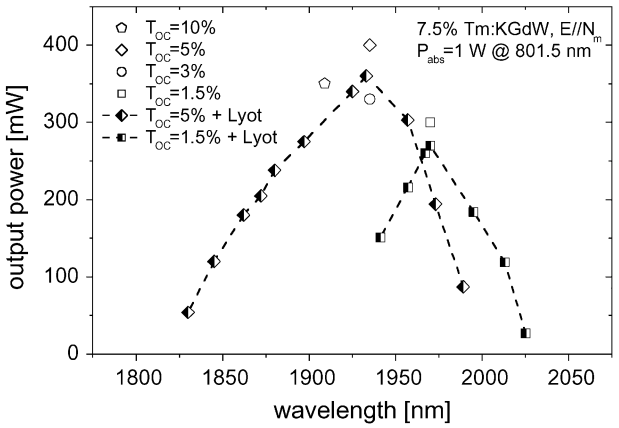

Fig. 9. Discrete tunability with the 7.5% Tm:KGdW sample for $E//N_m$, pumped at 801.5 nm achieved with $T_{\rm OC} = 1.5\%$ (half-filled squares) and 5% (half-filled diamonds). For comparison the generation wavelengths and output powers obtained without tuning element in the cavity are given for the four output couplers used (open symbols) and the same absorbed pump power $P_{\rm abs} = 1$ W.

results at this pump wavelength were essentially the same with respect to their dependence on $P_{\rm abs}$. The same is valid also for the 7.5% Tm-doped KGdW sample used for $E//N_m$ and pumped at 801.5 nm for which $P_{\rm abs} = 1$ W was achieved at a pump power of 1.15 W incident on L (Fig. 2). Specifically, with the $T_{\rm OC} = 5\%$ output coupler this sample provided a similar maximum output of 400 mW and a pump efficiency of 40% at $P_{\rm abs} = 1$ W. No essential differences in the output characteristics of the laser could be observed for pumping at slightly longer wavelengths (e.g., at 806 nm), better suited for laser diodes, the basic dependence being again on $P_{\rm abs}$.

In all cases discussed up to now, the laser linewidth was below our spectral resolution of 2 nm, achieved with a 60-cm monochromator, 600 l/mm grating and a PbS detector, but the laser wavelength was dependent on the sample, the orientation and the output coupler used. We attempted tuning by inserting a CaF_2 prism in the arm containing M1 (Fig. 2) or Lyot filters in the arm containing the output coupler M4. The prism with an apex angle of 69° was almost Brewster cut for 1900 nm and introduced only 10% reduction of the output power, however, its dispersion turned out to be insufficient for broad wavelength tuning. Note that flint type glasses on the other hand would introduce about 3% losses for a path of 10 mm at 1900 nm which makes them inappropriate for this laser.

We tried several Lyot filters (single and multiplate) but all of them were designed for operation in the visible and continuous tuning was difficult to achieve although their introduction into the cavity resulted also in ≈10% reduction of the output power. The best performance was observed with a 3-mm-thick quartz plate (diameter of 20 mm) whose optical axis was at 60° to the surface (this plate is described in detail in [29]). Quasi-continuous tuning is shown in Fig. 7 for $T_{\rm OC} = 1.5\%$ by the solid squares. Using different orders of the Lyot filter this tunability could be extended to shorter wavelengths and covered the 1816–2042 nm spectral range (half-filled squares in Fig. 7). The FWHM of 162 nm obtained for $T_{\rm OC} = 1.5\%$ is in principle capable of supporting sub-50-fs pulses near 1950 nm if this laser could be mode-locked.

As can be seen from Fig. 7 without the Lyot filter the laser wavelength continuously decreased with increasing the output coupling. Tuning in the case of $T_{\rm OC} = 10\%$ extended then the wavelength range down to 1790 nm at shorter wavelengths. Thus the output coupler had an essential influence on the tuning range achieved. Similar effects were observed also with the 5% Tm-doped sample cut for $E//N_P$ polarization (Fig. 8) and the 7.5% Tm-doped sample used at $E//N_m$ (Fig. 9). In both cases the wavelength exhibited jumps when exchanging the four output couplers. The reasons for these jumps can be traced back to the multiple minima in the wavelength dependence of the gain. While the gain cross section calculated in Fig. 6 can serve as a first approximation it does not take into account actual sample parameters.

We observed practically no change of the lasing wavelength from threshold up to the maximum output power for the 5%-doped sample and $E//N_m$. For the 5%-doped sample cut for $E//N_P$ only slight increase of the wavelength was observed reaching about 5 nm at maximum power

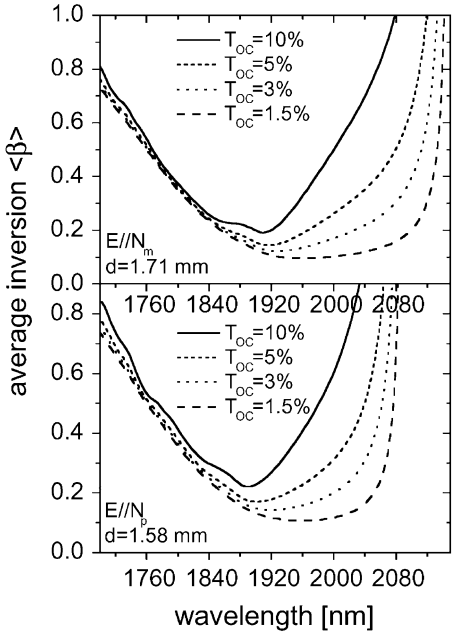

Fig. 10. Wavelength dependence of the average inversion $\langle\beta\rangle$ necessary to achieve threshold for the 5% Tm-doped KGdW samples with length d and different output couplers ($T_{\rm OC}$).

for $T_{\rm OC} = 10\%$. That is why it is justified to consider the wavelength dependence at threshold by equalizing the round trip losses ($T_{\rm OC}$) to the double pass gain. In contrast to the calculation of the gain cross section in Fig. 6 this allows an average inversion $\langle\beta\rangle = (1/d)\int_0^d \beta(z)dz$ necessary to achieve the threshold for a sample thickness d and Tm-ion density N to be estimated. In Fig. 10 the resulting $\langle\beta\rangle = (2\sigma_a Nd - \ln(1-T_{\rm OC}))/(2Nd(\sigma_a+\sigma_e))$ is plotted for the two samples with $N = 2.57\ 10^{20}$ ions/cm^3 Tm-concentration. While exact quantitave conclusions are difficult because additional losses are not accounted for (wavelength changes with $T_{\rm OC}$ make this impossible) two qualitative trends are seen in Fig. 10 that agree with our experimental observations. The wavelength jumps occur for both polarizations to shorter wavelengths when increasing $T_{\rm OC}$ and the wavelengths corresponding to minimum threshold at large $T_{\rm OC}$ are shorter for $E//N_P$ than for $E//N_m$.

In the case of $E//N_P$ (Fig. 8), the tunability range is shifted to shorter wavelengths and similar results as those depicted were obtained when pumping at 794 nm. As in the case of Fig. 7 the lower limit for the wavelength tuning was set unfortunately by the Lyot filter and not by the active medium itself. The similar output powers and tuning results obtained with the 7.5% Tm-doped sample (Fig. 9) indicate that there is no substantial quenching at this doping level in accordance with the fluorescence decay measurements [19].

The wavelength variations with the output coupling described just above preclude an accurate estimation of the total resonator losses. It is thus difficult to estimate the resonant (reabsorption) losses in the Tm:KGdW crystals because of the quasithree level system. On the other hand estimations of the nonresonant losses (by absorption or calorimetric methods) are still not available for the samples under investigation.

In the only work where tuning with Tm:KYW has been previously reported [21], with similar doping level and output coupling, the wavelength range from 1850 to 2004 nm could be covered. We extended this tuning range in the present work by $\approx$100 nm using the isostructural Tm:KGdW while the power levels achieved in the tuning mode exceed those from [21] about 8 times. It can be expected that with a more suitable Lyot filter and different cavity mirrors the tunability could be extended to below 1800 nm.

IV. Conclusion

In conclusion, we studied the potential of Tm:KGdW as a tunable 2-μm CW laser at room temperature. Besides the advantages in comparison to Tm:YAG or Tm:YLF outlined in the Introduction, it can be added that the tuning range is not only broader but also complementary to Tm:YAG and Tm:YLF at shorter wavelengths. The bandwidths supported by Tm:KGdW are pretty large so that mode-locking with passive methods (e.g., semiconductor saturable absorber) seems very promising. This should be possible by utilizing the same setup without additional cooling since the intracavity powers demonstrated ($>$ 25 W) are already very high. We are not aware of any CW passive mode-locking demonstration in any Tm-doped bulk medium up to now.

The further extension of the present results to yet higher output powers, is related on the other hand to the efficient heat removal from the active volume by a proper crystal holding construction. Note that the lower thermal conductivity of KGdW (see Table I) makes such materials predestined for highly efficient lasers in the low and medium (10 W) power regime. While the sample thickness used in the present work could be advantageous for utilizing the Kerr-effect self-mode-locking mechanism, thinner samples of higher doping level could further decrease the requirements to the spatial quality of diode based pump sources. It could be verified in the present work that doping levels of 7.5% have no degradation effect on the laser performance and on the basis of the spectroscopic results in [19] it can be expected that levels as high as 20% would be still feasible. The experiments with the tunable pump source permitted on one hand to compare pumping through different Stark levels, whose absorption lines depended on the polarization, on the other hand it could be confirmed that the use of conventional AlGaAs laser diodes should be uncritical both with respect to their (exact) wavelength and their linewidth.

We established that Tm:KGdW can operate also in the $E//N_P$ polarization although with lower efficiency. At present, it is unclear whether this could lead to some advantages in terms of bandwidth in the mode-locking regime but this polarization seems to provide higher gain at shorter wavelengths than $E//N_m$.

There are no reasons to conclude that Tm:KGdW possesses some intrinsic advantages over the isostructural Tm:KYW but such a comparison is planned for the near future. Improvements achieved here in comparison to previous laser work on Tm:KYW can be only attributed to superior crystal quality (e.g., suppression of nonradiative relaxation processes, an evidence for which is the relatively long fluorescence decay

time measured, see Table I), or the flexible resonator design and high mirror quality. That is why we conclude that all passive hosts belonging to the family of the monoclinic double tungstates are very promising materials for Tm-lasers.

REFERENCES

[1] D. N. Nikogosyan, *Properties of Optical and Laser-Related Materials: A Handbook*. New York: Wiley, 1997.

[2] S. A. Payne, L. L. Chase, L. K. Smith, W. L. Kway, and W. F. Krupke, "Infrared cross-section measurements for crystals doped with Er^{3+}, Tm^{3+}, and Ho^{3+}," *IEEE J. Quantum Electron.*, vol. 28, pp. 2619–2630, Nov. 1992.

[3] W. Ryba-Romanowski, "YVO_4 crystals—Puzzles and challenges," *Cryst. Res. Technol.*, vol. 38, pp. 225–236, June 2003.

[4] S. Golab, P. Solarz, G. Dominiak-Dzik,, T. Lukasiewicz, and W. Ryba-Romanowski, "Optical properties of YVO_4 crystals singly doped with Er^{3+}, Ho^{3+}, Tm^{3+}," *J. Alloys Compounds*, vol. 341, pp. 165–169, 2002.

[5] K. Ohta, H. Saito, and M. Obara, "Spectroscopic characterization of Tm^{3+}:YVO_4 crystal as an efficient diode pumped laser source near 2000 nm," *J. Appl. Phys.*, vol. 73, pp. 3149–3152, 1993.

[6] K. Ohta, H. Saito, M. Obara, and N. Djeu, "Characterization of a longitudinally pumped cw, room-temperature operation of Tm^{3+}-YVO_4laser," *Jpn. J. Appl. Phys.*, vol. 32, pp. 1651–1657, 1993.

[7] C. Hauglie-Hanssen and N. Djeu, "Further investigations of a 2-μm Tm:YVO_4 laser," *IEEE J. Quantum Electron.*, vol. 30, pp. 275–279, Feb. 1994.

[8] M. Bettinelli, F. S. Ermeneux, R. Moncorge, and E. Cavalli, "Fluorescence dynamics of YVO_4: Tm^{3+}, YVO_4:Tm^{3+}, Tb^{3+} and YVO_4:Tm^{3+}, Ho^{3+} crystals," *J. Phys.: Condens. Matter*, vol. 10, pp. 8207–8215, 1998.

[9] F. S. Ermeneux, C. Goutaudier, R. Moncorge, M. T. Cohen-Adad, M. Bettinelli, and E. Cavalli, "Growth and fluorescence properties of Tm^{3+} doped YVO_4 and Y_2O_3 single crystals," *Opt. Mat.*, vol. 8, pp. 83–90, 1997.

[10] C. Xueyuan and L. Zundu, "Spectroscopic characteristics, magnetic properties and fluorescence dynamics of Tm^{3+} in YVO_4 crystal," *J. Phys: Condensed Matter*, vol. 9, pp. 7981–7997, 1997.

[11] A. I. Zagumennyi, Yu. D. Zavartsev, P. A. Studenkin, V. I. Vlasov, I. A. Shcherbakov, C. P. Wyss, W. Luthy, H. P. Weber, and P. A. Popov, "Thermal conductivity of a Tm^{3+}:$GdVO_4$ crystal and the operational characteristics of a microchip laser based on it," *Quantum Electron.*, vol. 29, pp. 298–300, 1999. transl. from *Kvantovaya Elektronika*, vol. 27, pp. 16–18, 1999.

[12] L. J. Qin, X. L. Meng, H. Y. Shen, L. Zhu, B. C. Xu, L. X. Huang, H. R. Xia, P. Zhao, and G. Zheng, "Thermal conductivity and refractive indices of Nd:$GdVO_4$crystals," *Cryst. Res. Technol.*, vol. 38, pp. 793–797, 2003.

[13] Y. Urata, K. Akagawa, S. Wada, H. Tashiro, S. J. Suh, D. H. Yoon, and T. Fukuda, "Growth and optical properties of Tm:$GdVO_4$ single crystal," *Cryst. Res. Technol.*, vol. 34, pp. 41–45, 1999.

[14] A. A. Kaminskii, L. Li, A. V. Butashin, V. S. Mironov, A. A. Pavlyuk, S. N. Bagaev, and K. Ueda, "New stimulated emission channels of Pr^{3+} and Tm^{3+} ions in monoclinic $KR(WO_4)_2$ type crystals with ordered structure ($R = Y$ and Gd)," *Jpn. J. Appl. Phys.*, vol. 36, pp. L107–L109, 1997.

[15] S. N. Bagaev, S. M. Vatnik, A. P. Maiorov, A. A. Pavlyuk, and D. V. Plakushchev, "The spectroscopy and lasing of monoclinic Tm:$KY(WO_4)_2$," *Quantum Electron.*, vol. 30, pp. 310–314, 2000. (transl. from *Kvantovaya Elektronika*, vol. 30, pp. 310–314, 2000).

[16] A. A. Demidovich, A. N. Kuzmin, N. K. Nikeenko, A. N. Titov, M. Mond, and S. Kueck, "Optical characterization of Yb, Tm:KYW crystal concerning laser application," *J. Alloys Compounds*, vol. 341, pp. 124–129, 2002.

[17] M. I. V. Mochalov, "Laser and nonlinear properties of the potassium gadolinium tungstate laser crystal $KGd(WO_4)_2$:Nd^{3+}-(KGW:Nd)," *Opt. Eng.*, vol. 36, pp. 1660–1669, 1997.

[18] F. Güell, X. Mateos, J. Gavalda, R. Sole, M. Aguilo, F. Diaz, and J. Massons, "Blue luminescence in Tm^{3+}-doped $KGd(WO_4)_2$ single crystals," *J. Lumin.*, vol. 106, pp. 109–114, 2004.

[19] F. Güell, J. Gavalda, R. Sole, M. Aguilo, F. Diaz, M. Galan, and J. Massons, "1.48- and 1.84-μm thulium emissions in monoclinic $KGd(WO_4)_2$ single crystals," *J. Appl. Phys.*, vol. 95, pp. 919–923, 2004.

[20] C. Tu, J. Li, Z. Zhu, Z. Chen, Y. Wang, and B. Wu, "Spectra and intensity parameters of Tm^{3+}:$KGd(WO_4)_2$ laser crystal," *Opt. Commun.*, vol. 227, pp. 383–388, 2003.

[21] L. E. Batay, A. A. Demidovich, A. N. Kuzmin, A. N. Titov, M. Mond, and S. Kück, "Efficient tunable laser operation of diode-pumped Yb, Tm:$KY(WO_4)_2$ around 1.9 μm," *Appl. Phys. B*, vol. 75, pp. 457–461, 2002.

[22] L. E. Batay, A. N. Kuzmin, A. S. Grabtchikov, V. A. Lisinetskii, V. A. Orlovich, A. A. Demidovich, A. N. Titov, V. V. Badikov, S. G. Sheina, V. L. Panyutin, M. Mond, and S. Kück, "Efficient diode-pumped passively Q-switched laser operation around 1.9 μm and self-frequency Raman conversion of Tm-doped $KY(WO_4)_2$," *Appl. Phys. Lett.*, vol. 81, pp. 2926–2928, 2002.

[23] S. M. Vatnik, E. Balashov, A. A. Pavljuk, E. Golikova, and A. Lyutetskiy, "Measurement of gain and evolution of photon avalanche efficiency in 10% Tm:$KY(WO_4)_2$ crystal pumped by free-running Nd:YAG laser," *Opt. Commun.*, vol. 220, pp. 397–400, 2003.

[24] S. M. Vatnik, A. P. Maiorov, A. A. Pavlyuk, and D. V. Plakushchev, "Spectroscopy and kinetics of the population of monoclinic $KYb_{0.5}Y_{0.43}$ $Tm_{0.07}$ $(WO_4)_2$ crystals pumped by a pulsed Nd:YAG laser," *Quantum Electron.*, vol. 31, pp. 19–22, 2001. (transl. from *Kvantovaya Elektronika*, vol. 31, pp. 19–22, 2001).

[25] F. Güell, X. Mateos, J. Gavalda, R. Sole, M. Aguilo, F. Diaz, M. Galan, and J. Massons, "Optical characterization of Tm^{3+}-doped $KGd(WO_4)_2$ single crystals," *Opt. Mat.*, vol. 25, pp. 71–77, 2004.

[26] C. Tu, J. Li, Z. Zhu, Y. Wang, Z. You, B. Wu, and B. Alain, "Crystal growth of $KGd(WO_4)_2$:Tm^{3+}," *J. Cryst. Growth*, vol. 256, pp. 63–66, 2003.

[27] B. M. Walsh, N. P. Barnes, and B. Di Bartolo, "Branching ratios, cross sections, and radiative lifetimes of rare earth ions in solids: Applications to Tm^{3+} and Ho^{3+} ions in $LiYF_4$," *J. Appl. Phys.*, vol. 83, pp. 2772–2787, 1998.

[28] M. C. Pujol, X. Mateos, R. Sole, J. Massons, J. Gavalda, F. Diaz, and M. Aguilo, "Linear thermal expansion tensor in KRE $(WO_4)_2$(RE= Gd, Y, Er, Yb) monoclinic crystals," *Materials Science Forum*, vol. 378–381, pp. 710–715, 2001.

[29] M. Wittmann, A. Penzkofer, and W. Bäumler, "Generation of frequency tunable femtosecond pulses in a cw pumped linear dispersion-balanced passive mode-locked rhodamine 6-G dye laser," *Opt. Commun.*, vol. 90, pp. 182–192, 1992.

Valentin Petrov was born in Plovdiv, Bulgaria, in 1959. He received the M.Sc. degree in nuclear physics from the University of Sofia, Sofia, Bulgaria, in 1983 and the Ph.D. degree in optical physics from the Friedrich–Schiller University, Jena, Germany, in 1988.

He joined the Max-Born-Institute for Nonlinear Optics and Ultrafast Spectroscopy in Berlin, Germany, in 1992. His research interests include ultrashort light pulses, laser physics, and nonlinear optics and he has coauthored about 130 papers in scientific journals.

Frank Güell was born in Vila-Rodona, Spain in 1973. He received the B.Sc. degree in physics from Barcelona University, Barcelona, Spain, in 1998. He is currently working toward the Ph.D. degree in physics at the Rovira i Virgili University (U.R.V.), Tarragona, Spain.

Jaume Massons was born in Lleida, Spain, in 1959. He received the Ph.D. degree in physics from Barcelona University, Barcelona, Spain, in 1987.

He is currently a Senior Lecturer of Applied Physics at the Rovira i Virgili University (U.R.V.), Tarragona, Spain. His research interests include optical spectroscopy of rare-earth ions for laser applications and nonlinear optical processes.

Josefina Gavalda received the Ph.D. degree in physics from Barcelona University, Barcelona, Spain, in 1989.

Currently, she is a Senior Lecturer of Applied Physics at the Rovira i Virgili University (U.R.V.), Tarragona, Spain. She is working on optical spectroscopy of rare-earth ions for laser applications and also on the morphological characterizations of several materials based in scanning electron microscopy.

Rosa Maria Sole was born in Tarragona, Spain, in 1965. She received the Ph.D. degree in physics from Barcelona University, Barcelona, Spain, in 1994.

She is currently a Lecturer of Applied Physics at the Rovira i Virgili University (U.R.V.), Tarragona, Spain. Her research interests include phase diagrams, crystals growth, and physical properties of the solutions and crystals.

Magdalena Aguilo was born in Mallorca, Spain, in 1953. She received the Ph.D. degree in physics from Barcelona University, Barcelona, Spain, in 1983.

Currently, she is Professor of Crystallography. Her research interests include crystal growth, X-ray diffraction, X-ray texture analysis, and physical properties in relation with the crystalline structure.

Francesc Diaz was born in Lugo, Spain, in 1953. He received the Ph.D. degree in physics from Barcelona University, Barcelona, Spain, in 1982.

Currently, he is Professor of Applied Physics at the Rovira i Virgili University (U.R.V.), Tarragona, Spain. His research interests include optical spectroscopy (absorption and emission) of rare-earth ions for laser applications and nonlinear optical processes, such as cooperative luminescence and step-up conversion.

Uwe Griebner received the Ph.D. degree in physics from the Technical University of Berlin, Berlin, Germany in 1996. His Ph.D. research was on fiber bundle lasers with high average power.

Since 1992 he has been with the Max-Born-Institute in Berlin, Germany, working on diode-pumped solid-state lasers, fiber lasers, waveguide lasers, microoptics, microoptics for special resonators, and ultrafast lasers. He is currently focused on ultrafast diode-pumped solid-state lasers and amplifiers applying new active materials and the use of micro-optical components for femtosecond beam-shaping.